DOE/ER/14386-1

BI-FUNCTIONAL AIR ELECTRODES FOR METAL-AIR BATTERIES

FINAL REPORT

for Period September 15, 1993 - December 14, 1994

by

Larry L. Swette, Mourad Manoukian and Anthony B. LaConti

Giner, Inc.
14 Spring Street
Waltham, MA 02154

December 1995

Prpared for

U.S. Department of Energy
Office of Energy Research
9800 South Cass Avenue
Argonne, IL 60439

Grant DE-FG02-93ER14386.M001

NOTICE

ABSTRACT

The program was directed to the need for development of **bifunctional air electrodes** for Zn-Air batteries for the consumer market. The Zn-Air system, widely used as a primary cell for hearing -aid batteries and as a remote-site power source in industrial applications, has the advantage of high energy density, since it consumes oxygen from the ambient air utilizing a thin, efficient fuel-cell-type gas-diffusion electrode, and is comparatively low in cost. The disadvantages of the current technology are a relatively low rate capability, and the lack of simple reversibility. "Secondary" Zn-Air cells require a third electrode for oxygen evolution or mechanical replacement of the Zinc anodes; thus the development of a bifunctional air electrode (i.e., an electrode that can alternately consume and evolve oxygen) would be a significant advance in Zn-Air cell technology.

Evaluations of two carbon-free non-noble metal perovskite-type catalyst systems, $LaNiO_3$ and $La_{1-x}Ca_xCoO_3$ as bifunctional catalysts for potential application in Zn-air batteries were carried out. The technical objectives were to develop higher-surface-area materials and to fabricate reversible electrodes by modifying the hydrophobic/hydrophilic balance of the catalyst-binder structures.

TABLE OF CONTENTS

LIST OF TABLES AND FIGURES

I. INTRODUCTION

A. Summary of Results

This program was directed to the need for development of **bifunctional air electrodes** for Zn-Air batteries for the consumer market. The Zn-Air system is widely used as a primary cell for hearing -aid batteries and as a remote-site power source in industrial applications. The Zn-Air cell has the advantage of high energy density, since it consumes oxygen from the ambient air utilizing a thin, efficient fuel-cell-type gas-diffusion electrode, and is comparatively low in cost. The disadvantages of the current technology are a relatively low rate capability, and the lack of simple reversibility. "Secondary" Zn-Air cells require a third electrode for oxygen evolution or mechanical replacement of the Zinc anodes; thus the development of a bifunctional air electrode (i.e., an electrode that can alternately consume and evolve oxygen) would be a significant advance in Zn-Air cell technology.

The specific goal of the program was to evaluate two carbon-free non-noble metal perovskite-type catalyst systems, namely **$LaNiO_3$** and **$La_{1-x}Ca_xCoO_3$** as bifunctional catalysts for potential application in Zn-air batteries. The technical objectives were to develop higher-surface-area materials and to fabricate reversible electrodes by modifying the hydrophobic/hydrophilic balance of the catalyst-binder structures. The following results were obtained:

- $LaNiO_3$ catalyst surface areas were increased by factors of 2 to 4 over traditional preparation methods,
- $LaNiO_3$ electrodes typically showed very high rate oxygen evolution (charge) performance without apparent detriment to catalyst composition,
- Some $LaNiO_3$ electrodes exhibited good short-term oxygen reduction (discharge) performance,
- All electrode compositions, both for $LaNiO_3$ and $La_{1-x}Ca_xCoO_3$, exhibited a characteristic decay in performance on discharge coincident with a drastic shift in wettability from balanced hydrophobic pre-test to "flooded" post-test.

B. Background

The main obstacle to the development of a bifunctional oxygen electrode is the incompatibility of most oxygen reduction catalysts with oxygen evolution conditions. Typical oxygen reduction catalysts (Pt, Au, Ag, Co-macrocyclics, carbon) are not stable at oxygen evolution potentials; they exhibit dissolution to various degrees which can be detrimental to the zinc electrode, and they can suffer surface area loss due to particle growth. Similarly, typical oxygen evolution catalysts perform poorly for oxygen reduction, and noble metals can be detrimental to the zinc electrode. Carbon, a good support and an oxygen reduction catalyst in alkaline medium, is not stable in the oxygen evolution environment (Ross and Sokol, 1984). A highly graphitized form has been reported to give improved stability (Ross, 1990), but the polarization performance for O_2 reduction may be compromised because of modified surface properties (Scherson, et al., 1991)

A true bifunctional electrode requires that all components be capable, at a minimum, of withstanding the complete range of the electrochemical potential environment imposed by the applied load and recharge regimen. Ideally, the catalytic component(s) should also be capable of depolarizing both the oxygen reduction and evolution reactions. Such a bifunctional-catalyst/ single-electrode structure is anticipated to be the most efficient and cost-effective oxygen electrode for an electrically rechargeable metal-oxygen battery, and was therefore selected as the operational model in this development program.

C. Technical Approach

Two carbon-free non-noble metal perovskite-type catalyst systems were proposed for evaluation as bifunctional catalysts for use in Zn-air batteries for the consumer market. **$LaNiO_3$** has been studied by several investigators and is generally reported to be a promising candidate bifunctional catalyst. This perovskite-type oxide has been truly tested in both oxidation and reduction mode. Kannan, et al. (1989) show a performance of 0.9 V vs. RHE for O_2 reduction (30 mA/cm^2) and 1.53 V for evolution (100 mA/cm^2). They do not mention any problems with stability, although no cycle life test data is given in this paper. Matsumoto and co-workers (1977a) also report good performance over the period of a week but indicate that there is a potential stability problem below about 0.55 V vs. RHE. Swette and Kackley (1990) found through corrosion current measurements and post-test analyses that the $LaNiO_3$ is stable in the potential range of 0.6 to 1.6 V (RHE). Another perovskite-type oxide that has recently been reported to show promise as a bifunctional catalyst is **$La_{1-x}Ca_xCoO_3$** (Shimizu, et al., 1990). This material has been prepared with moderate surface area (17 m^2/g) and is apparently stable over the bifunctional potential range; the electrical conductivity is not reported and the test results are compromised by the inclusion of carbon for the electrode structure. Two shortcomings are typically observed for these materials: 1) all synthesis methods reported yield a relatively low-surface-area powder, and 2) most electrode structures are not suitable for bifunctional operation; many rely on carbon for the structure and fail prematurely. Substantial improvements need to be made to reduce particle size and achieve higher surface areas than are typically obtained for traditional synthesis methods, and bifunctional electrode structures need to be developed. These improvements were the focus of this study.

The objectives of this study were:

1) **investigation of preparation methods to achieve higher-surface-area $LaNiO_3$ and $La_{1-x}Ca_xCoO_3$, and**

2) **fabrication of unique Integrated Dual-Character electrodes that are carbon-free and optimized for bifunctional operation in a Zn-Air battery,**

3) **demonstration of extended bifunctional operation in a reversible oxygen cell.**

The first objective was met in that higher-surface-area materials were successfully synthesized but, in spite of a broad and intensive effort, no electrode fabrication technique yielded a catalyst-binder structure that retained its initial balanced hydrophobic/hydrophilic character after brief discharge operation, even at the extremes of initial hydrophobicity. This phenomenon prevented further development or extended practical bifunctional testing of the candidate catalysts.

II. EXPERIMENTAL METHODS AND PROCEDURES

A. Catalyst Syntheses

Relatively high-surface-area perovskite-type oxides were synthesized by modification of two methods, the classical hydroxide co-precipitation of metal salts and the more recently developed amorphous citrate precursor method. The modifications tried were as follows:

Modifications to the Hydroxide Method

Precursor Modifications:

pH adjustment of the metal nitrate solutions to "imminent precipitation" before addition to the hydroxide for optimum co-precipitation

Addition of hypochlorite and wetting agent to the hydroxide solution to ensure metal ion oxidation (Vidyasagar, et al; 1985)

Freeze-drying of the co-precipitated precursor for increased surface area.

Conversion Modifications:

Temperature and time variations

Addition of "sintering interferants"

Modifications to the Amorphous Citrate Precursor Method

Freeze drying of the precursor before conversion

Conversion temperature and time variations.

1. Preparation from the Hydroxide Co-Precipitated Precursor (HCP)

Equal volumes of 1M La and Ni nitrate solutions were mixed and 0.1M sodium hydroxide solution was added to adjust the pH to 5.1 to bring the metal ions to the point of imminent precipitation. The pH change curves are shown in **Figure 1**. An appropriate amount of 6M NaOH solution (slightly more than the stoichiometric requirement) was placed in a separate beaker and, to provide oxidizing conditions to ensure oxidation of the metal ions, 2 ml of NaOCl (4.6% available chlorine) was added along with 1 ml. of 5% Triton-X 100 surfactant, according to the method of Vidyasagar, et al. (1985). The metal nitrate mix was then added dropwise to the constantly stirred hydroxide solution along with 2 ml of NaOCl solution added 0.1 ml at a time. The co-precipitated hydroxide mix was centrifuged and washed alkali free several times with distilled water until the pH of the solution was ~7. The hydroxide precursor was dried in air at 100°C for 2 hours. The precursor was converted to $LaNiO_3$ by firing under O_2. One preparation (N463-35) was freeze-dried after co-precipitation. This yielded a very low density, "fluffy" precursor, but the BET surface area was actually lower than non-freeze-dried preparations.

2. Preparation from the Amorphous Citrate Precursor (ACP)

Amorphous citrate precursors were synthesized according to the method of Zhang, et al (1987). 3M solutions of La and Ni nitrates were prepared and mixed with 6M aqueous solution of citric acid. The molar ratio of citric acid to **total** metal cations was fixed at unity. Water

was evaporated from the mixed solution using freeze-drying apparatus until a sol was obtained. The sol was further dehydrated at around 70°C for 4 hours in a vacuum oven to yield a dry "foam" of the amorphous precursor. Conversion to $LaNiO_3$ was performed by careful heating in air.

3. Conversion of the Precursors to Perovskites

To gain some understanding of the mechanisms of decomposition and to determine the likely range of conditions required for the preparation of $LaNiO_3$, the thermal reaction behavior of the precursors was examined by means of Thermogravimetric Analysis (TGA). Thermogravimetric analyses were conducted in 30% O_2, 70% N_2 at Microtherm in Weston, MA. The samples were heated from room temperature up to a maximum of 1000°C at a rate of 10°C/min.

The TGA curve for an hydroxide precursor (Sample #N463-29[H]) is shown in **Figure 2**. The La-Ni hydroxide exhibits thermal reactions at three points: 200-270°C, 300-360°C and 450-690°C. The decomposition steps correspond to weight losses of 4.5, 5.5 and 4.5 percent, respectively. No weight loss was observed above 690°C. Conversion of the hydroxide precursors was typically accomplished by heating the dried powders under oxygen in a tube furnace at different temperatures and for different durations, typically longer times for lower temperatures. In order to preserve the surface area of the precursor, the addition of a "sintering interferant" was also investigated. The objective was to prevent growth of the crystals and agglomeration of the particles by adding a non-reactive material to the precursor in a large excess (e.g., a 10 to 1 ratio) to keep the precursor particles separated during thermal conversion. The material selected for this function was sodium carbonate, which proved to be non-reactive and could be effectively washed out with hot water after thermal conversion.

TheTGA results for the decomposition of the amorphous citrate precursor are presented in **Figure 3**. ACP sample #N463-28[ACP] was found to undergo decomposition in two steps, 120-210°C and 210-320°C. At around 320°C, which corresponds to the second decomposition step, the precursor loses ~92% of its starting weight and the results are not valid above this point. Decomposition of the amorphous citrate precursors was performed in a muffle furnace in air. Because of the rapid exothermic decomposition reaction of amorphous citrate precursors at 320°C, the temperature was increased stepwise through the critical temperature point. X-ray diffraction analysis indicated that it was necessary to continue heating to much higher temperatures to achieve conversion to $LaNiO_3$.

The conversion conditions used in each of the preparations are listed in **Table 1**.

B. Characterization of Catalyst Powders

The electrical conductivity and surface area were typically measured for all powder preparations; in some cases the surface area of the precursor was measured also to track the change on conversion. The values obtained for each preparation are listed in Table 1. Selected samples were submitted for x-ray diffraction analysis to determine crystal structure and phase purity. Some samples were also examined by electron microscopy to evaluate particle size and agglomeration.

Table 1. Preparation Parameters and Properties of $LaNiO_3$ and $LaCaCoO_3$ Catalysts

Serial No.	Amount Prepared (g)	Sintering Interferant	Conversion Temp. (°C)	Conversion Time (hr)	Metal Oxide Resistivity @ 3000 psi (ohm-cm)	Surface Area (m^2/g)
N450-91[H]	2.4	---	400	6	Non-Conduct.	9.8
N450-91A[H]	1.5	---	400/600	6/6	3.2	10.3
N450-92[H]	4.8	---	400	6	Non-Conduct.	50.4
N450-92A[H]	2.0	---	400/600	6/6	4.6	20.4
N450-94[H]	8.0	---	800	6	1.7	8.7
N463-17[H]	10.0	---	---	---	---	52.1
N463-17-21[H]	3.9	Na_2Co_3	800	6	1.7	9.2
N463-17-28A[H]	3.0	Na_2Co_3	700	6	3.2	14.0
N463-17-28B[H]	3.0	---	700	6	3.6	14.6
N463-29[H]	10.0	---	---	---	---	59.8
N463-29-40[H]	5	---	700	6	0.20	13.5
N463-35[H]	9.0	---	---	---	---	19.2
N463-35-40[H]	5	---	700	6	0.08	6.1
N463-40[H]	10	---	700	6	---	---
N463-29-66[H]	5	Na_2Co_3	700	6	---	---
N463-68[H]	10	---	700	9	5.1	17.0
N463-69[H]	10	---	700	6	4.2	8.8
N463-77[H]	5	---	650	16	7.8	19.0

Serial No.	Amount Prepared (g)	Sintering Interferant	Conversion Temp. (°C)	Conversion Time (hr)	Metal Oxide Resistivity @ 3000 psi (ohm-cm)	Surface Area (m^2/g)
N463-18[ACP]	9.6	---	650	2	9.8	1.9
N463-28[ACP]	9.0	---	---	---	---	0.33
N463-28-30A[ACP]	0.20	---	650	2.5	---	15.2
N463-28-30B[ACP]	0.60	---	700	2.5	2.3	9.6
N463-28-32[ACP]	2.0	---	650	2.5	1.31	14.6
N463-28-33[ACP]	2.0	---	650	2.5	---	13.0
N463-69-71[ACP]	3	---	400	4	N/C	5.7
N463-69-72[ACP]	3	---	500	4	N/C	6.0
N463-69-73[ACP]	3	---	700	2.5	3.6	12.5
N463-75[ACP]	5	Na_2CO_3	700	3.5	2.9	8.5
N463-75[ACP]	5	---	800	5	2.8	8.3
N463-85$LaCaCoO_3$						
N463-85A[ACP]	5	---	600	4	3.1	14
N463-85B[ACP]	5	---	700	4	3.2	14

[H]: Prepared by Hydroxide Precursor Method
[ACP]: Prepared by Amorphous Citrate Method

1. Electrical Conductivity

The electrical conductivity of the catalyst powders was determined using a four probe method. A schematic of the holder used for the conductivity measurements is shown in **Figure 4**. A current of 200 mA was passed through the ends of the bed of catalyst powder. The potential drop measured between the probes was used to calculate resistivity.

2. Surface Area

The surface areas of the catalyst powders were measured by the B.E.T. nitrogen adsorption/desorption technique (Brunauer, et al; 1938) using an in-house Micromeretics Flow Sorb II 2300 instrument.

3. X-Ray Diffraction Analysis

The catalyst powders were characterized by x-ray powder diffraction (XRD) initially at University of Connecticut by Professor Bert Chamberland, and later at Orion Research Laboratories in N.Y to determine the phase and crystalline structure of the catalyst powders.

4. Transmission Electron Microscopy

Transmission Electron Microscopy (TEM) was performed at IEA laboratories in Billerica, MA. Standard copper grids were coated with a thin layer of catalyst particles, dried and then positioned in the microscope. Photomicrographs were obtained at a magnification of 78,000x.

C. Fabrication of Electrodes

The gas-diffusion electrodes investigated were fabricated as a catalyst layer (perovskite only, no carbon) mixed with a polytetrafluoroethylene binder (Dupont Type 30 Teflon dispersion) pressed on to a nickel mesh (Exmet 5Ni5-5/0) backed by a porous PTFE film (Goretex sheet with 1 micron pores). The finished electrodes were processed at 350^{0}C for 20 minutes. The catalyst loading was targeted at 20 to 40 mg/cm^2.

Several different methods were investigated to prepare the catalyst/binder mix. During the course of this development it was found that electrodes prepared by "wet casting" were easier to fabricate in small sizes and generally exhibited better performance. In wet casting, a few milliliters of distilled water were added to the catalyst powder followed by a measured amount of Teflon dispersion, ranging from 15 to 60 wt%. The critical process of catalyst-Teflon particle association was found to be difficult to achieve with the perovskite materials. The most successful method appeared to be mechanical stirring with high shear conditions. This was achieved by transferring the catalyst-Teflon mix to a tall graduate cylinder and stirring at a high rate for an extended period with a plastic rod of slightly smaller diameter than the graduated cylinder. The exact amount of Teflon seemed to be somewhat less important than the process of catalyst-Teflon particle association; above about 35 wt% , however, the electrodes showed increased electrical resistivity. The resulting mix would settle to the bottom of the graduate cylinder on standing leaving a clear supernatant, suggesting the desired particle association. Mixes prepared in this manner were then poured ("wet cast") on to the porous PTFE sheet laid over a sintered glass vacuum filtration funnel;

the porous PTFE sheet with the catalyst-binder layer was laid over a nickel mesh, pressed, dried and then heated in air at 350 ^{0}C for 20 minutes.

In another approach the catalyst-Teflon mix was prepared as a well-mixed thick paste and the shearing action was introduced by rolling. This paste was placed between two thin sheets of Teflon and rolled several times in all directions. The resulting thin layer of catalyst-binder was then pressed on to a Ni mesh, dried and sintered.

Dry powder methods, tried initially, were generally unsuitable and were not pursued in depth.

D. Electrochemical Characterization of Electrodes

The electrodes were evaluated as one cm^2 samples in a "floating electrode" cell (Giner and Smith; 1967) as shown in **Figure 5**. The counter electrode was a nickel mesh around the inner glass cylinder. The apparatus was equipped with thermocouple and temperature controllers. Oxygen/air was passed through a saturator before entering into the cell. The cell temperature was maintained at 40 ^{0}C. The electrolyte was 30% KOH solution and was continuously stirred during the measurements with a small magnetic stirring bar. The potential of the working electrode was changed stepwise with a PAR potentiostat using a dynamic hydrogen electrode (DHE) as the reference electrode (Giner; 1964). The resulting current density was measured and recorded at each applied potential. Electrodes that performed well in oxygen were also tested in air. The wettability of each electrode before and after electrochemical characterization was determined by visual observation of the contact angle and distribution of water placed on the surface.

III. RESULTS AND CONCLUSIONS

A. Physical Properties of Perovskite Catalysts $LaNiO_3$ and $La_{1-x}Ca_xCoO_3$

The preparation parameters and physical properties of the perovskite catalysts were summarized in **Table 1**. The Hydroxide Coprecipitation Process yielded precursors with surface areas in the range of 50 to 60 m^2/g. Low temperatures of conversion were explored initially (prior to TGA evaluation of the precursors) to preserve as much of this surface area as possible. Catalyst samples N450-91(H) and N450-92(H) were heated at 400°C for 6 hours but the resulting oxide was non-conductive, indicating incomplete conversion of the hydroxide precursor. Both samples were heat treated for an additional 6 hours in O_2 at 600°C. Conductivity values could then be measured and XRD analysis indicated that sample N450-92A(H) was single phase $LaNiO_3$. The effects of time, temperature and the use of a sintering interferant are summarized in **Table 2**. As would be expected, higher temperatures yielded materials with lattice parameters closer to the literature values but lower in surface area. The use of the sintering interferant, sodium carbonate, yielded material with closely matched lattice parameters (indicating the absence of reactivity), but did not preserve surface area as hoped. Overall the best results both in terms of surface area and electrode performance were obtained by thermal conversion at 600°C for 12 hours.

Table 2. X-Ray Diffraction Analysis of HCP Preparations of $LaNiO_3$

PREPARATION CONDITIONS			LATTICE PARAMETERS			BET S. A.
Method	**Temp(°C)**	**Time (hrs)**	**a**	**c**	**Vol (Å)^3**	**(m^2/g)**
	Literature Values →		5.448	13.12	337.3(2)	5-15
HCP	800	6	5.479	13.31	346.1(4)	8.7
HCP	700	6	5.487	13.29	346.4(8)	14.6
HCP/SI*	700	6	5.443	13.22	339.2(5)	14.0
HCP	400/600	6/6	5.509	13.18	346.3(5)	20.4

* SI = Sintering Interferant (Na_2CO_3)

The $LaNiO_3$ powders prepared by the amorphous citrate precursor (ACP) method generally showed lower surface areas than those prepared by the HCP method, even though the freeze-drying process yielded a promising voluminous precursor. Powder diffraction patterns were recorded for four samples prepared by the ACP method. The precursors were processed at 400, 500, 700 and 800°C. The XRD patterns for powders prepared at 400 and 500°C, shown in **Figures 6 and 7**, indicate the absence of $LaNiO_3$. At 700°C (**Figure 8**) three species were detected; $La_2O_2CO_3$, NiO and $LaNiO_3$. The sample prepared by heating at 800°C for 5 hours (**Figure 9**) appeared to be pure single phase $LaNiO_3$ but had a low surface area, 8.3 m^2/g.

Electron microscopic examination of some of the catalyst preparations was performed to examine particle morphology for the presence of any microstructure and to determine whether particle agglomeration (resulting in another level of microporosity) was occurring since these phenomena might account for the unusual persistent degradation of the hydrophobic properties of the electrodes when tested. TEM micrographs of catalyst powders are shown in **Figures 10 to 17**. It can be seen that the particles are generally crystalline in structure and vary in shape and size (correlating to some extent with measured BET surface area) but show no obvious signs of microporosity. Most of the micrographs suggest that agglomeration could be occuring, however. Such agglomerates of particles, if they are stable, could exhibit microporosity that would interfere with the normal catalyst/binder association at the particulate level resulting in electrodes that exhibit superficial hydrophobicity but retain a strong capillary force in the agglomerate microstructure. TEM micrographs taken of the HCP precursors (**Figures 18 and 19**) suggest that agglomeration was probably occuring at this stage which would account for the relative ineffectiveness of the sintering interferant. TEM micrographs of the ACP samples (**Figures 15 to 17**) show that the catalysts prepared by the ACP method have much larger particles compared to the catalyst powders prepared by the HCP method; this is also consistent with surface area measurements.

A TEM micrograph of an electrode surface (**Figure 20**) reveals some porosity in several large particles, not observed in the powder micrographs, that would be anticipated to resist wet-proofing with Teflon and might present a more hydrophilic character than estimated from the simple ratio of Teflon to catalyst.

B. Electrode Performance Testing

Nearly 50 experimental electrodes were fabricated by a variety of techniques in the course of the program but , as stated earlier, all electrodes exhibited the same flooding phenomenon on testing, the only variation being the rate of degradation. This is of course detrimental to the oxygen reduction discharge reaction. The transient discharge data obtained indicate that both $LaNiO_3$ and $La_{1-x}Ca_xCoO_3$ are catalytically active, however. The performance on charge was typically quite good (oxygen evolution would tend to benefit from a more flooded structure), suggesting catalytic activity for this reaction also and stability under oxidizing conditions. The possibility of a chemical change after electrochemical testing of the electrode was addressed by sending a sample of the catalyst powder for x-ray diffraction analysis after bifunctional testing in KOH. **Figure 21** shows the XRD pattern of the catalyst powder. Major components of the sample were identified as pure $LaNiO_3$ by comparing the diffraction pattern to the Joint Conference on Powder Diffraction Standards (JCPDS) library.

The effect of electrode structure on performance is illustrated in **Figure 22** for a single catalyst compounded with four different levels of Teflon binder, all fabricated by the "rolling" process. It can be seen that the oxygen evolution polarization is relatively constant but the transient oxygen reduction polarization is significantly influenced by the electrode wettability. The best performance data for some representative catalysts and electrode structures are presented in **Figures 23 to 27**. The best bifunctional performance was obtained with an electrode fabricated, by the "wet cast" process, from an HCP preparation of $LaNiO_3$ converted at low temperature (400^0C/ 6 hrs + 600^0C/6 hrs); this sample (N450-92A[H]) had the highest surface area, 20.4 m^2/g (**Figure 25**). If this material could be prepared as finer discrete particles with less agglomeration, it might lend itself to the necessary catalyst-PTFE association at the particulate level to permit the formation of an acceptable balanced, stable hydrophobic/hydrophilic structure suitable for cyclic oxygen reduction-evolution; such a material could be a viable candidate for an economical bifunctional positive electrode for the Zn-Air cell.

Catalysts prepared by the ACP method, both $LaNiO_3$ and $La_{1-x}Ca_xCoO_3$, generally showed lower performance (**Figures 26 and 27**) and do not show any obvious promise of improved properties or performance that would justify this substantially more difficult and time consuming synthesis method.

IV. REFERENCES

Brunauer, S., Ph. Emmett, E. Teller, *J. Am. Chem. Soc.*, **60**, 309 (1938).

Giner, J., "A Practical Reference Electrode," *J. Electrochem. Soc.*, **111**, 376-7 (1964).

Giner, J., and S. Smith, *Electrochemical Technology*, **5**, 59-61 (1967).

Kannan, A.M., A.K. Shukla, S. Sathyanarayana, "Oxide-Based Bifunctional Oxygen Electrode for Rechargeable Metal/Air Batteries," *J. Power Sources*, **25**, 141-50 (1989).

Matsumoto, Y., H. Yoneyama, H. Tamura, "Influence of Preparation Condition on Catalytic Activity for Oxygen Reduction of Lanthanum Nickel Oxide and Related Oxides," *J. Electroanal. Chem.*, **83**, 167-76, (1977a).

Matsumoto, Y., H. Yoneyama, H. Tamura, "Electrochemical Properties of Lanthanum Nickel Oxide," *J. Electroanal. Chem.*, **80**, 115-21, (1977b).

Ross, P.N., and H. Sokol, *J. Electrochem. Soc.*, **131**, 1742 (1984).

Ross, P.N., "Novel Air Electrode for Metal-Air Battery With New Carbon Material and Method of Making the Same," U.S. Patent No. 4,927,718 (1990).

Scherson, D., D. Tryck, M. Daroux, X. Xing (Eds.), "Recommendations of the Study Panel Concerning Future Directions for Research on Oxygen Electrochemistry," Proceedings of the Workshop on Structural Effects in Electrocatalysis and Oxygen Electrochemistry, Oct. 29-Nov. 1, 1991, Cleveland OH.

Shimizu, Y., K. Uemura, H. Matsuda, N. Miura, N. Yomazoe, "Bi-Functional Oxygen Electrode Using Large Surface Area $La_{1-x}Ca_xCoO_3$ for Rechargeable Metal-Air Battery," *J. Electrochem. Soc.*, **137**(11), 3430-33 (1990).

Swette, L., and N. Kackley, "Oxygen Electrodes for Rechargeable Alkaline Fuel Cells - II," *J. Power Sources*, **29**, 423-36 (1990).

Swette, L., N. Kackley, S.A. McCatty, "Oxygen Electrodes for Rechargeable Alkaline Fuel Cells - III," *J. Power Sources*, **36**, 323-339 (1991).

Vidyasagar, K., J. Gopalakrishnan, C.N.R. Rao, "Synthesis of Complex Metal Oxides Using Hydroxide, Cyanide, and Nitrate Solid Solution Precursors," *J. Solid State Chem.*, **58**, 29-37 (1985).

Zhang, H-M., Y. Teraoka, N. Yamazoe, "Preparation of Perovskite-Type Oxides with Large Surface Areas by Citrate Process," *Chemistry Letters*, p. 665 (1987).

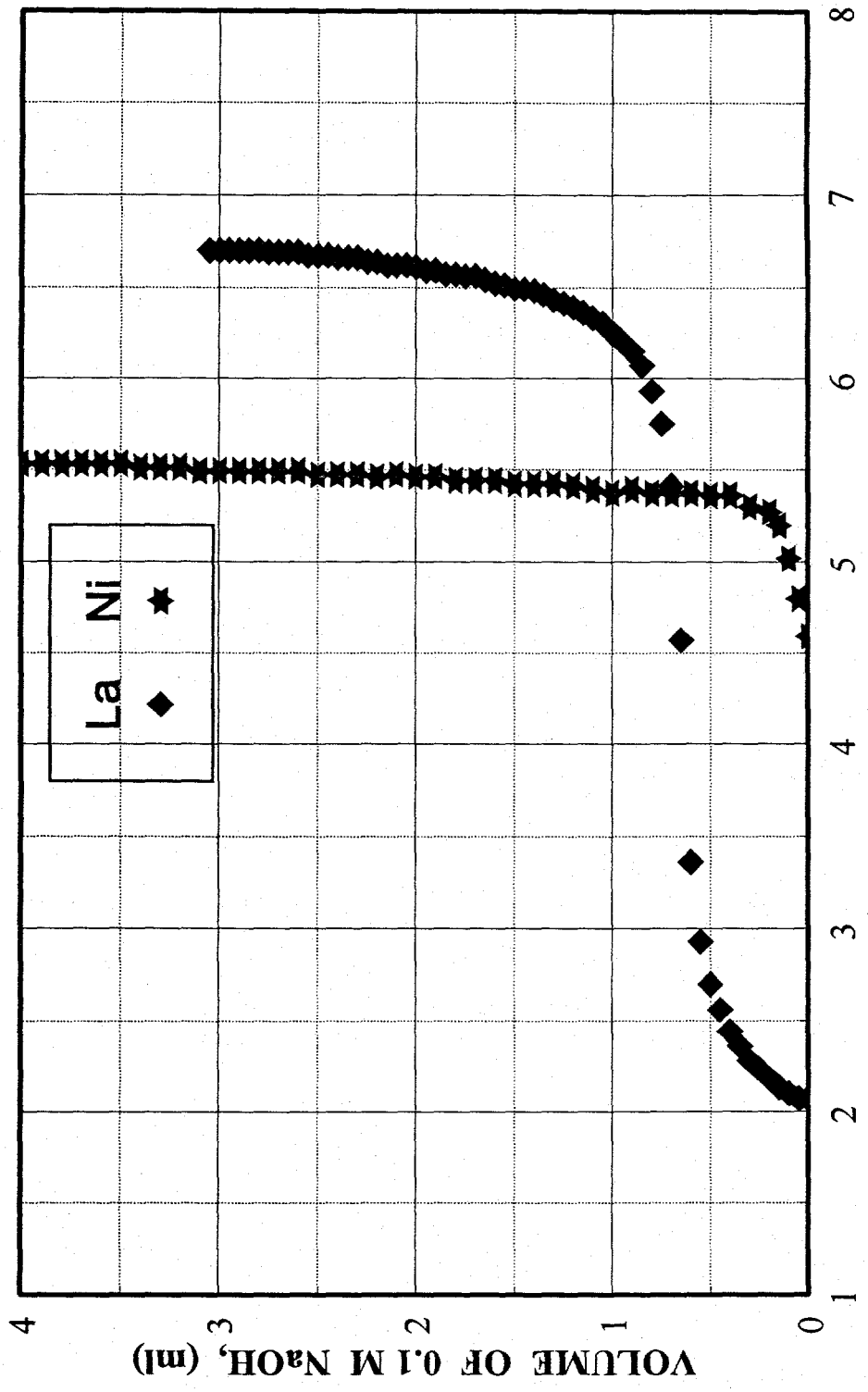

Figure 1. Titration Curves for 1M $Me(NO_3)_x$, where Me = La, Ni

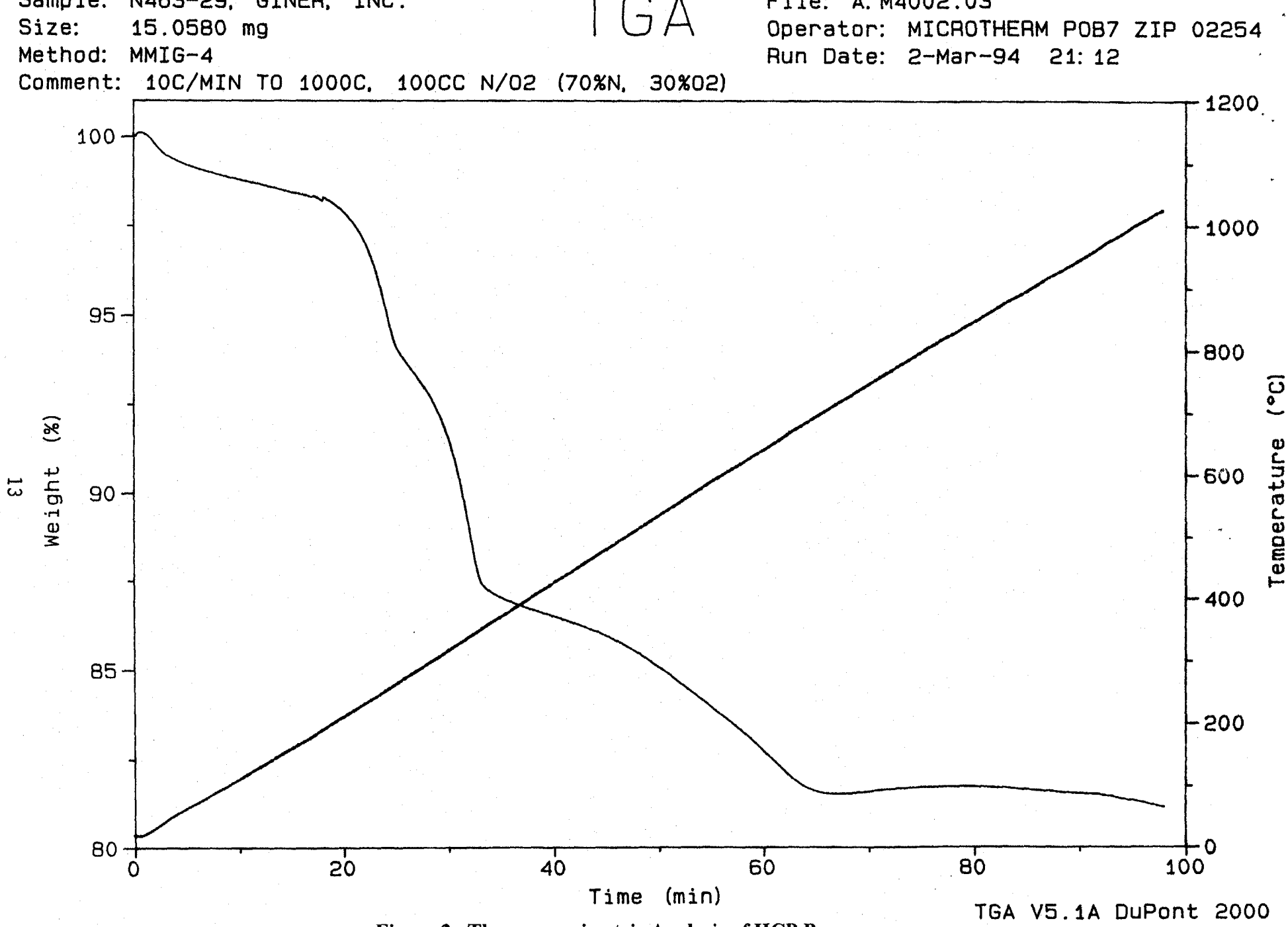

Figure 2. Thermogravimetric Analysis of HCP Precursor

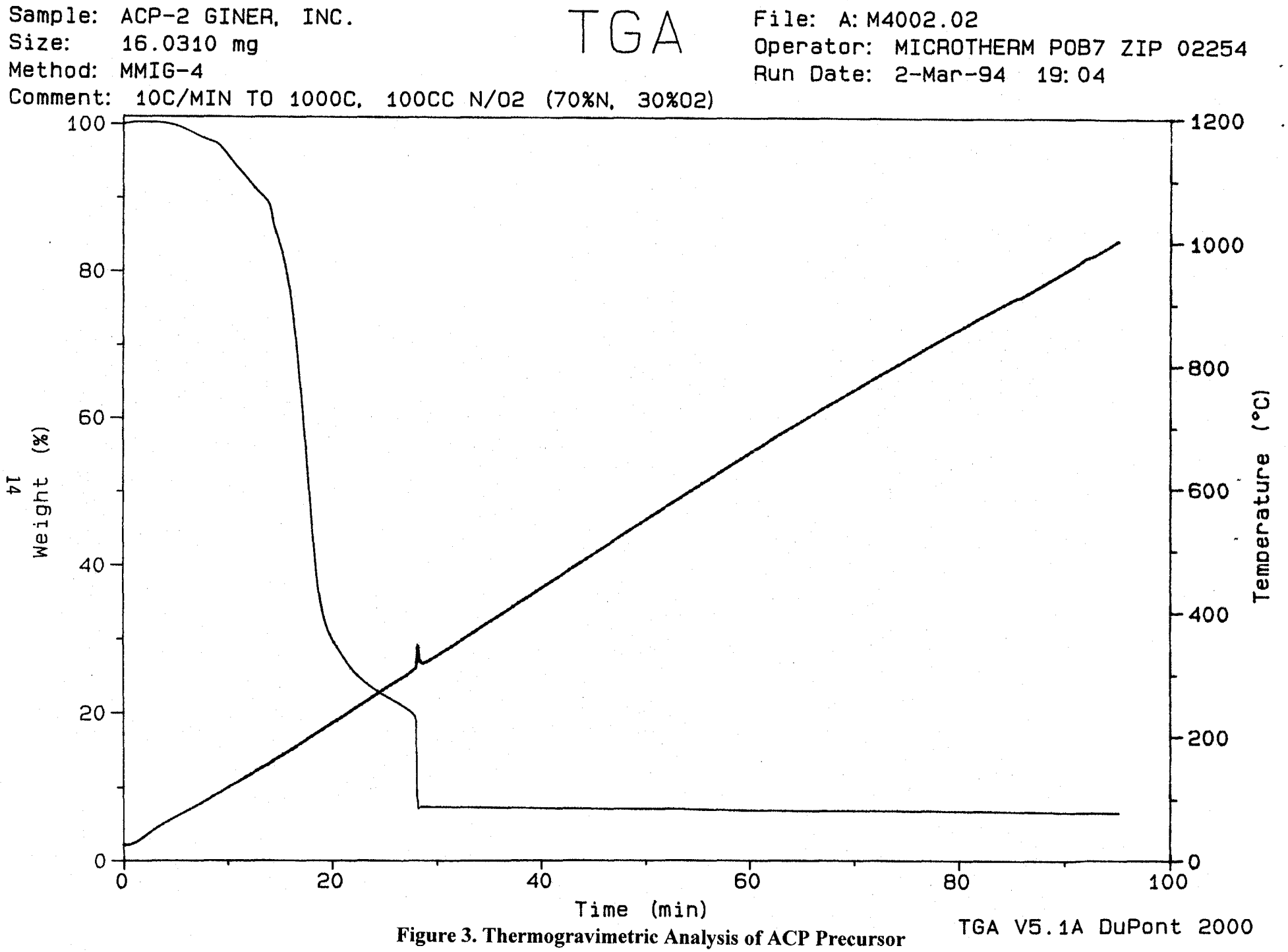

Figure 3. Thermogravimetric Analysis of ACP Precursor

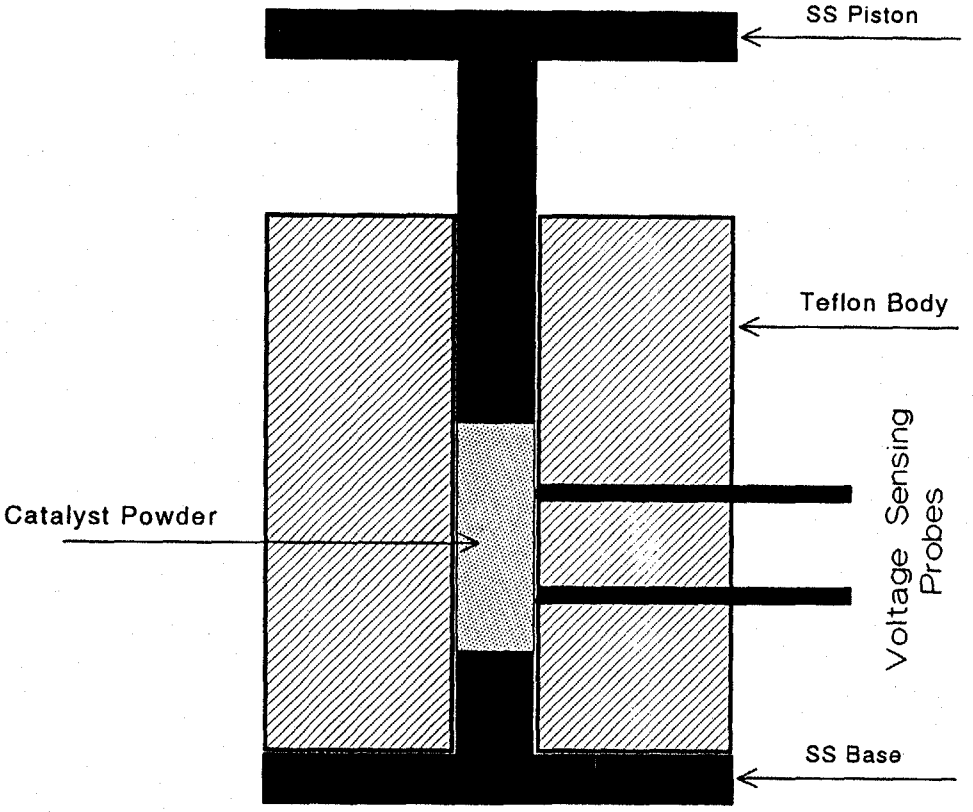

Figure 4. Holder for Four-Probe Conductivity Measurements

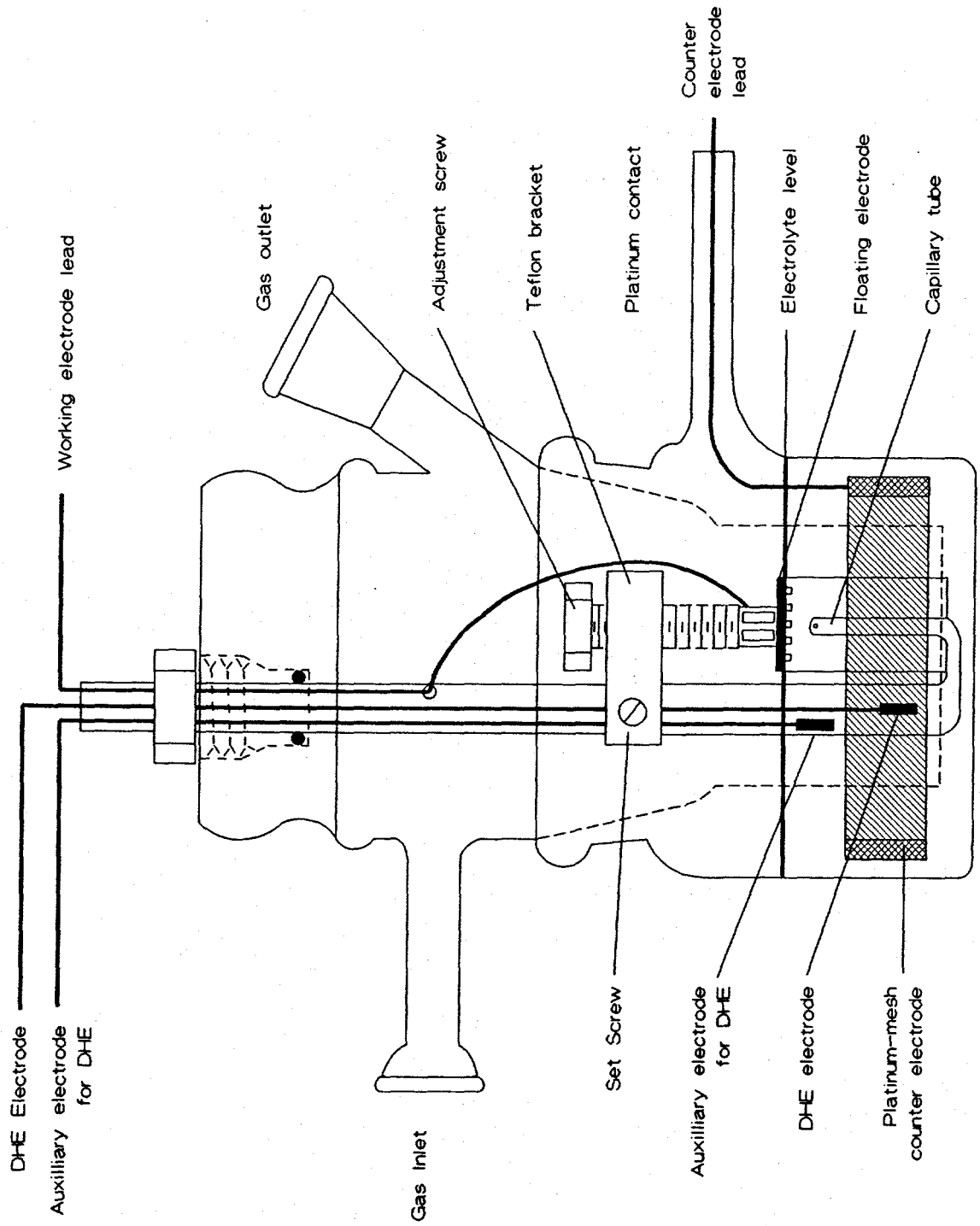

Figure 5. Floating Electrode Cell (diagram)

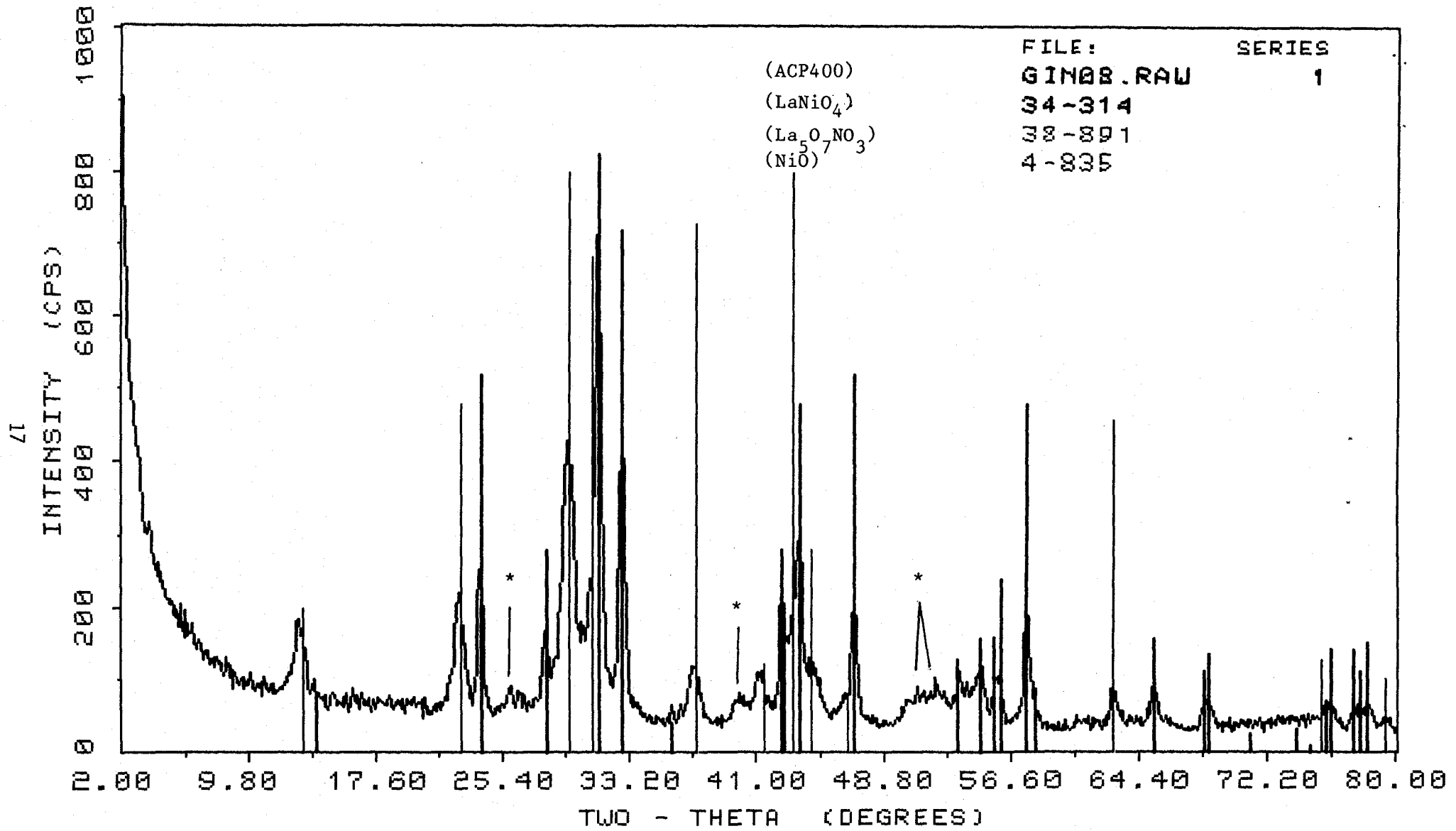

Figure 6. X-Ray Diffraction Pattern for ACP $LaNiO_3$, Heated 4 Hours at 400° C (N463-69-71)

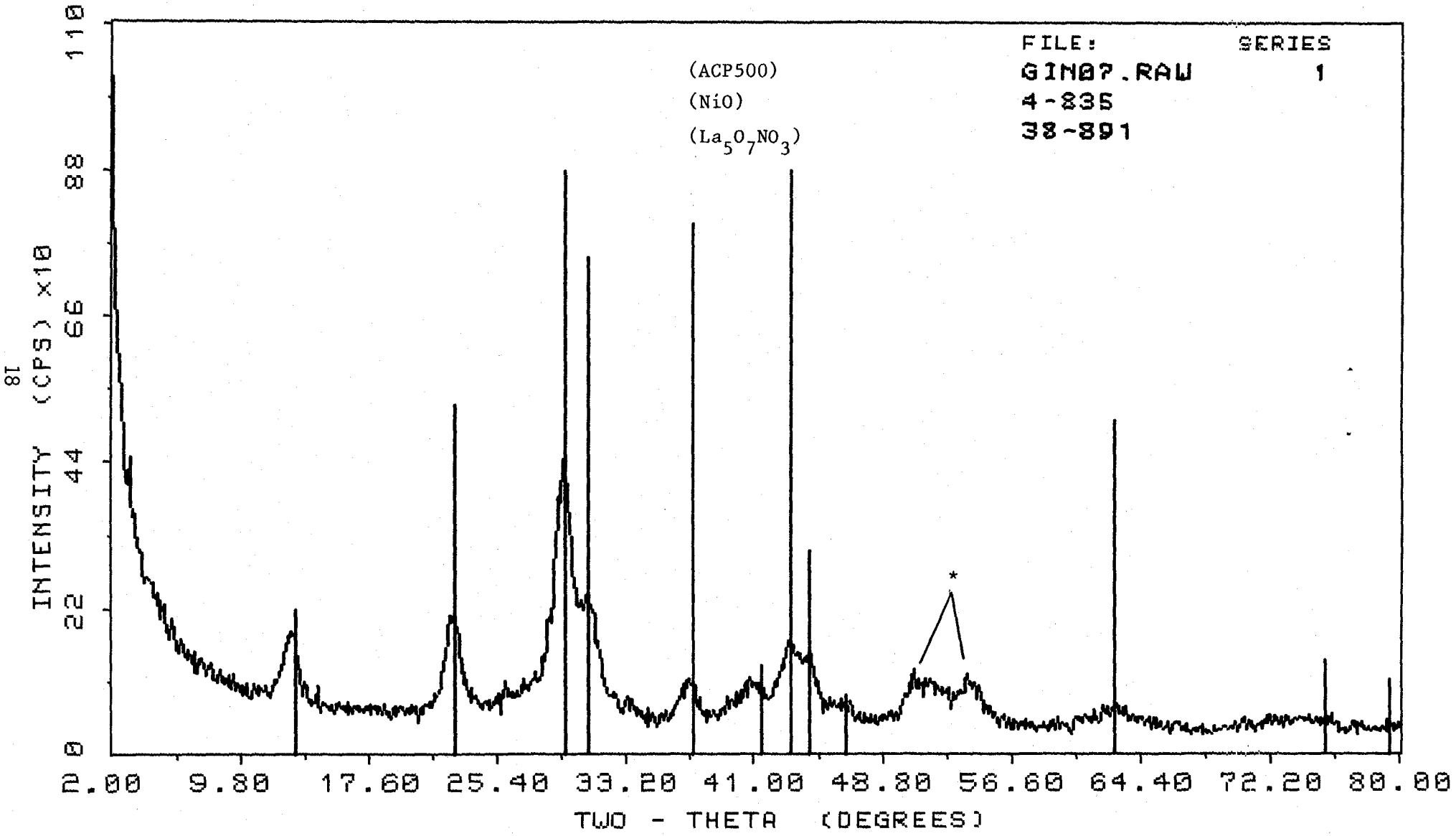

Figure 7. X-Ray Diffraction Pattern for ACP $LaNiO_3$, Heated 4 Hours at 500° C (N463-69-72)

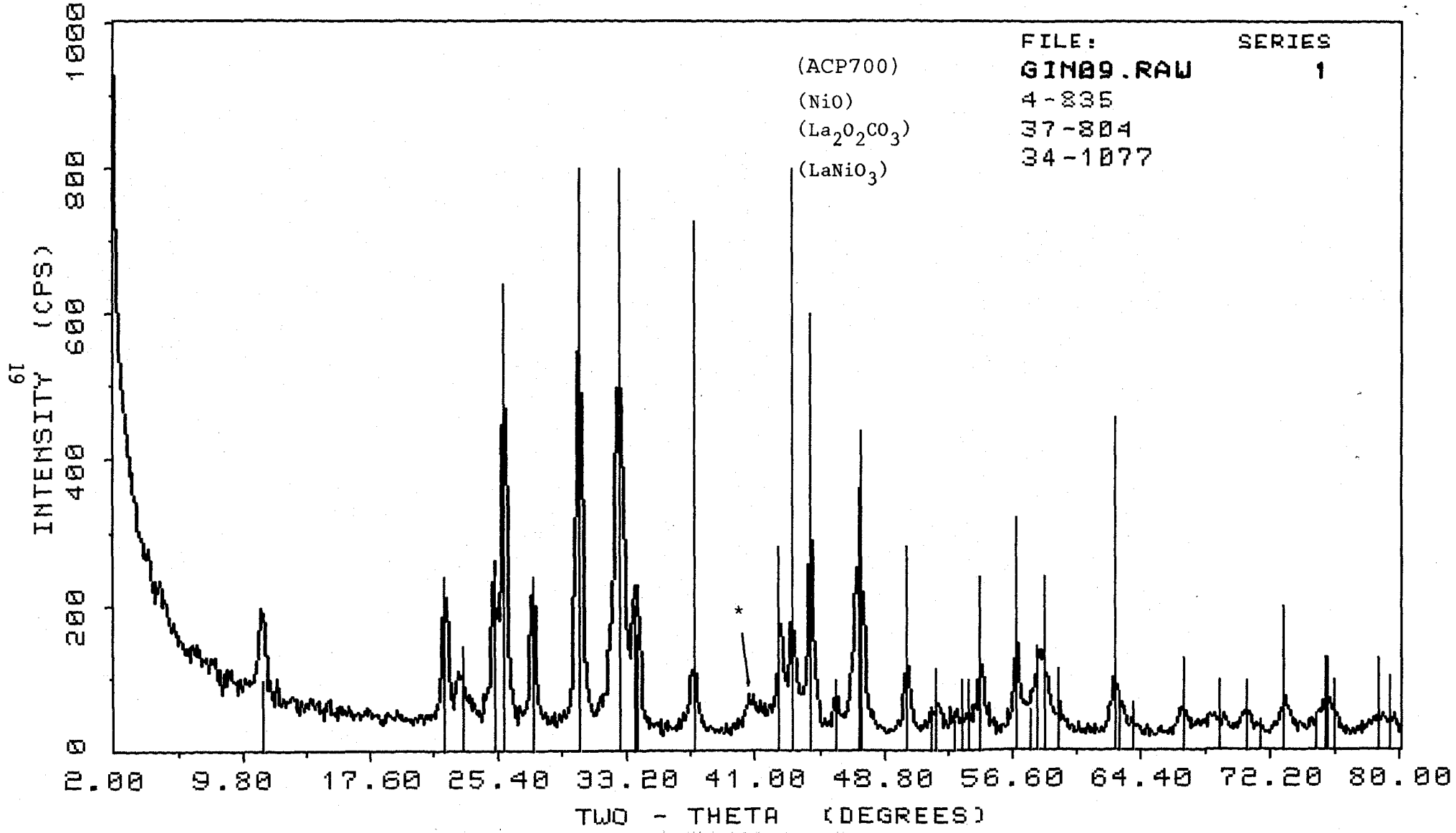

Figure 8. X-Ray Diffraction Pattern for ACP $LaNiO_3$, Heated 2.5 Hours at 700° C (N463-69-73)

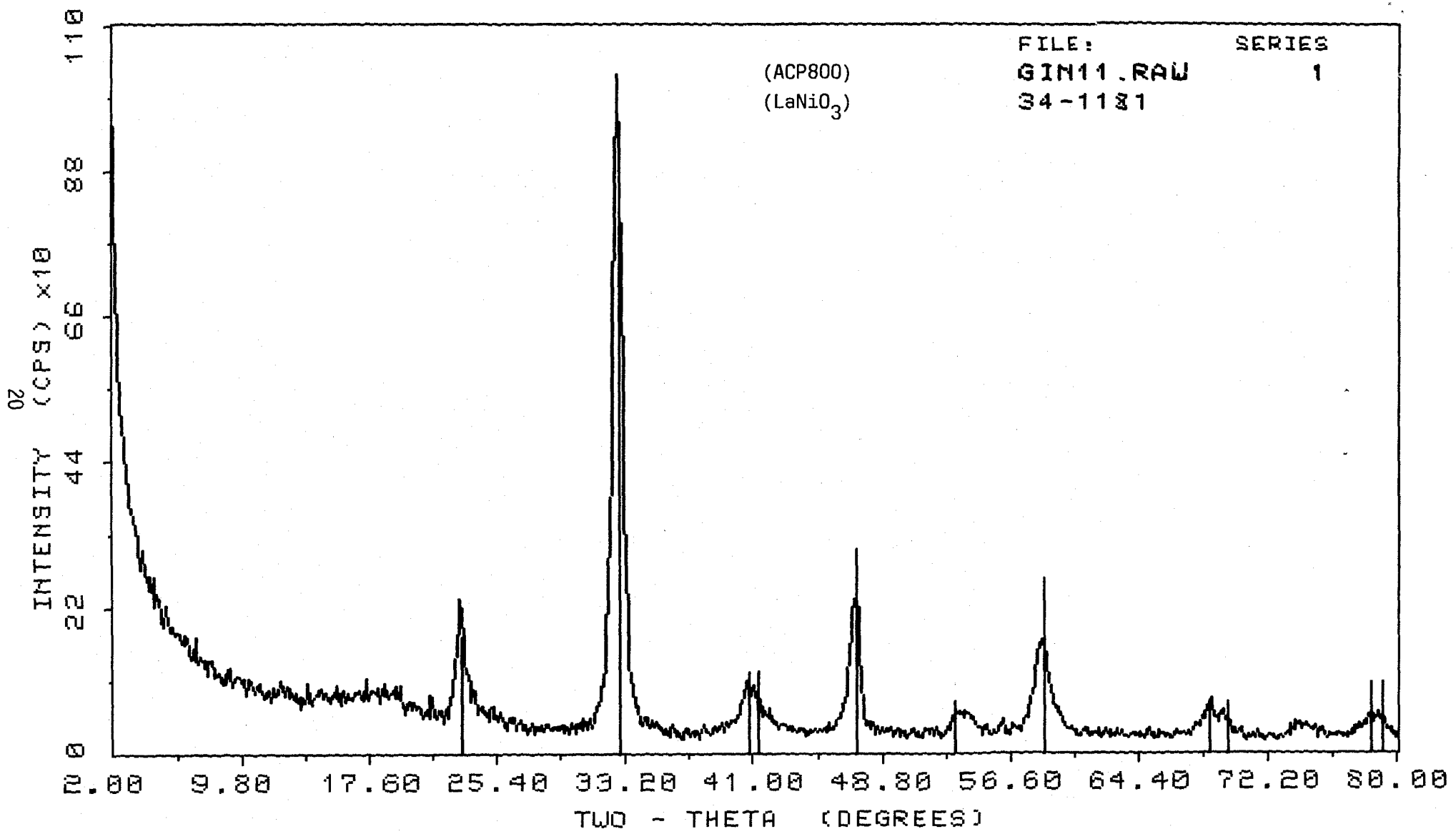

Figure 9. X-Ray Diffraction Pattern for ACP $LaNiO_3$, Heated 5 Hours at 800° C (N463-75)

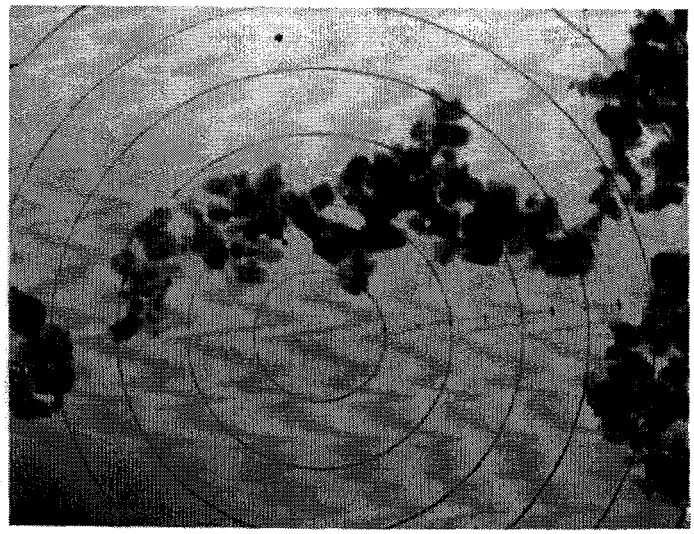

Figure 10. TEM @ 78,000x, $LaNiO_3$, HCP Process, 400°C/6 hrs + 600°C/6 hrs; 20.4 m^2/g (N450-92A)

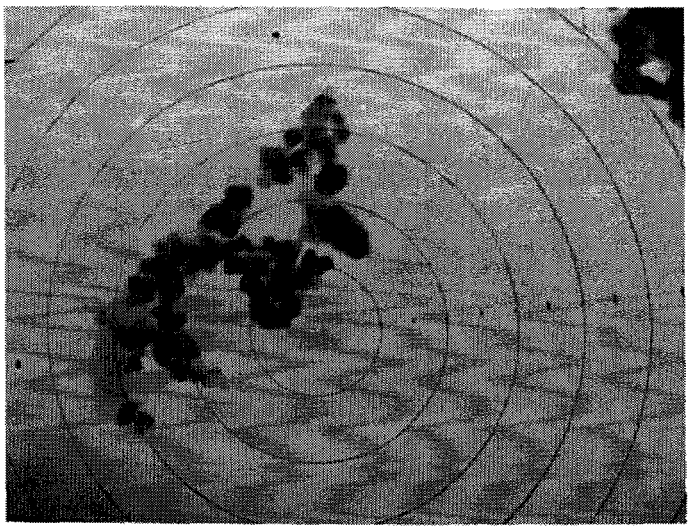

Figure 11. TEM @ 78,000x, $LaNiO_3$, HCP Process, 700°C, 6 hrs; 14.6 m^2/g (N463-17-28B)

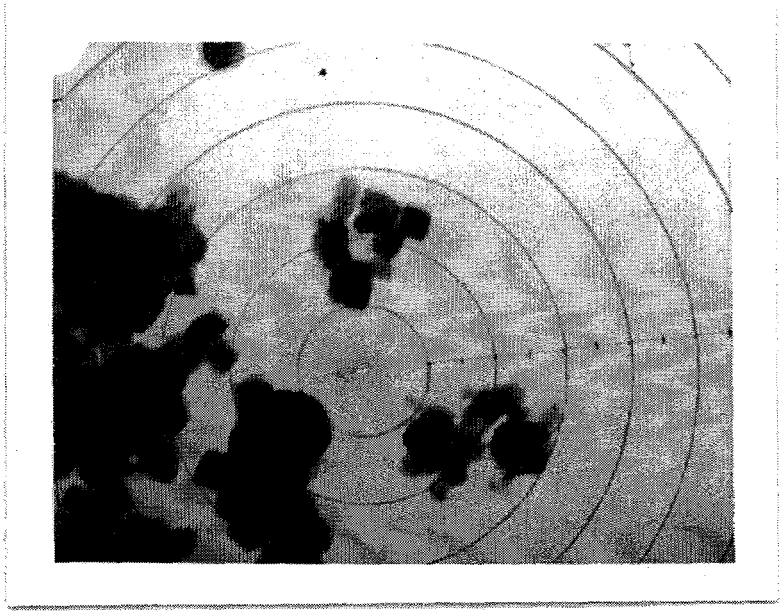

Figure 12. TEM @ 78,000x, $LaNiO_3$, HCP Process, 700°C, 6 hrs, with Na_2CO_3 as Sintering Interferant; 14 m^2/g (N463-17-28A)

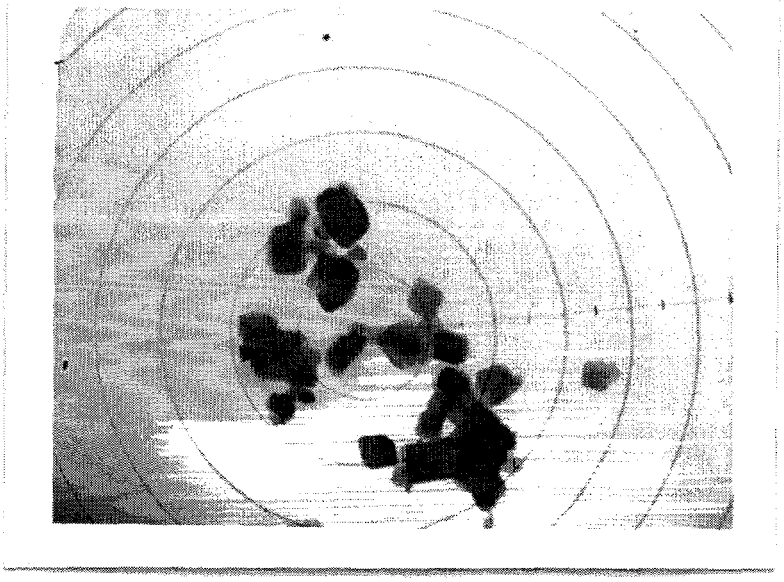

Figure 13. TEM @ 78,000x, $LaNiO_3$, HCP Process, 800°C, 6 hrs; 8.7 m^2/g (N450-94)

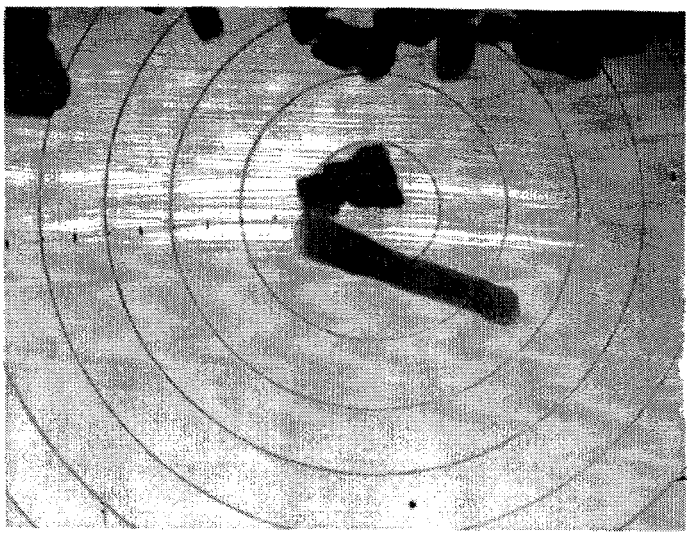

Figure 14. TEM @ 78,000x, $LaNiO_3$, HCP Process, 800°C, 6 hrs, with Na_2CO_3 as Sintering Interferant; 9.2 m^2/g (N463-17-21)

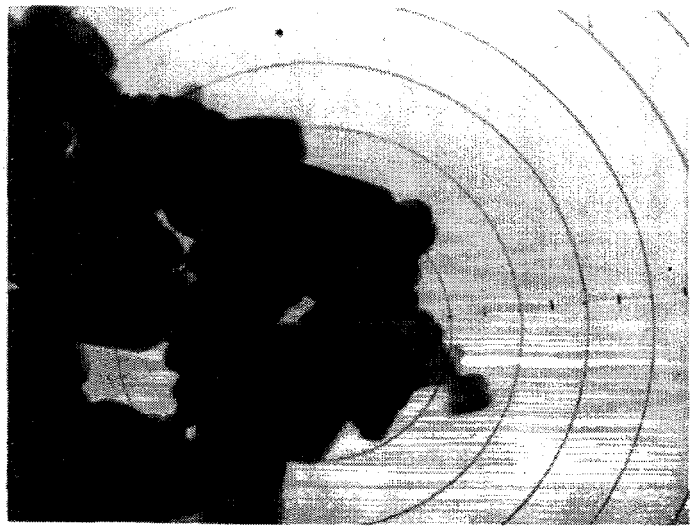

Figure 15. TEM @ 78,000x, $LaNiO_3$, ACP Process, 600°C, 2 hrs; 1.9 m^2/g (N463-18)

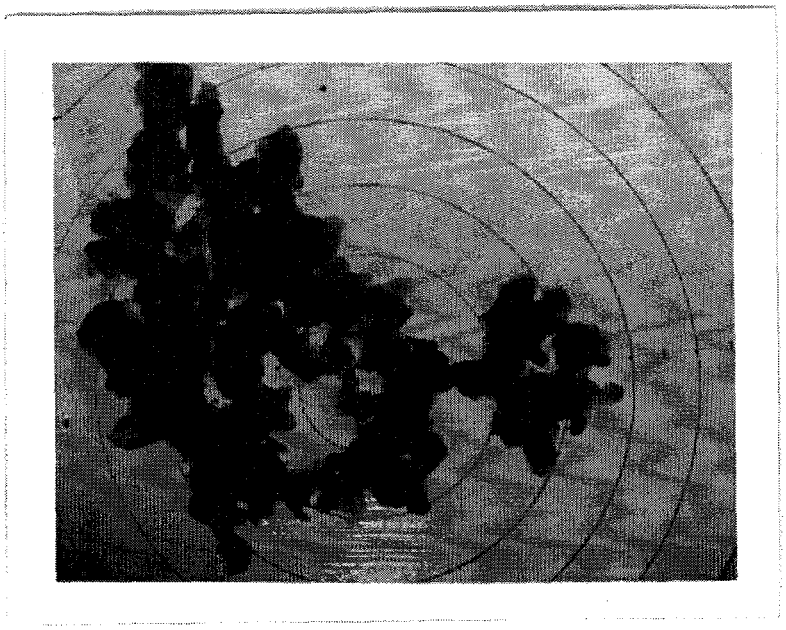

Figure 16. TEM @ 78,000x, $LaNiO_3$, ACP Process, 650°C, 2.5 hrs; 13 m^2/g (N463-78-33)

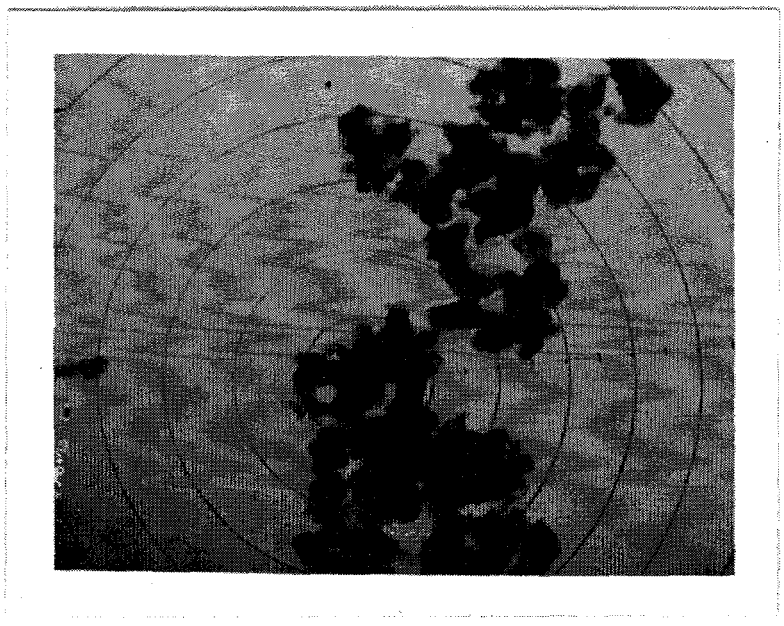

Figure 17. TEM @ 78,000x, $LaNiO_3$, ACP Process, 700°C, 2.5 hrs; 9.6 m^2/g (N463-28-30B)

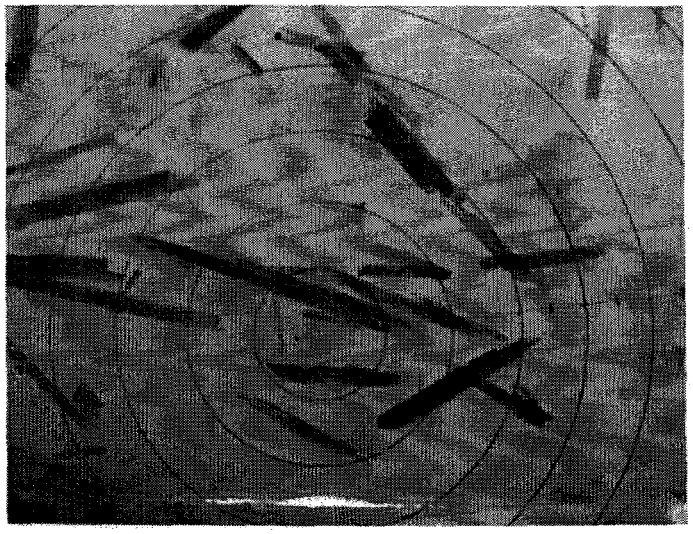

Figure 18. TEM @ 78,000x, HCP Process, Precursor Powder; 59 m^2/g (N463-29)

Figure 19. TEM @ 78,000x, HCP Process, Freeze-Dried Precursor Powder; 19.2 m^2/g (N463-35)

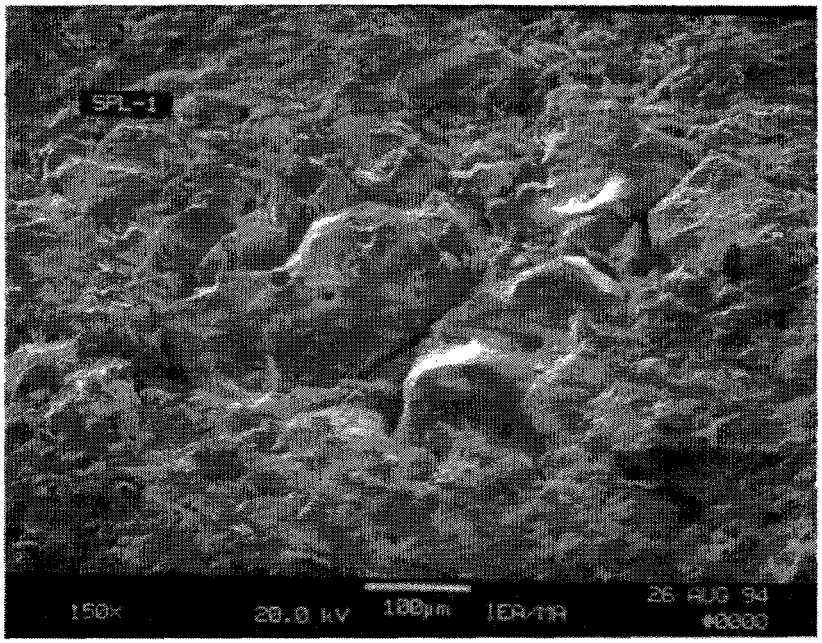

Figure 20. TEM of $LaNiO_3$ Electrode Surface

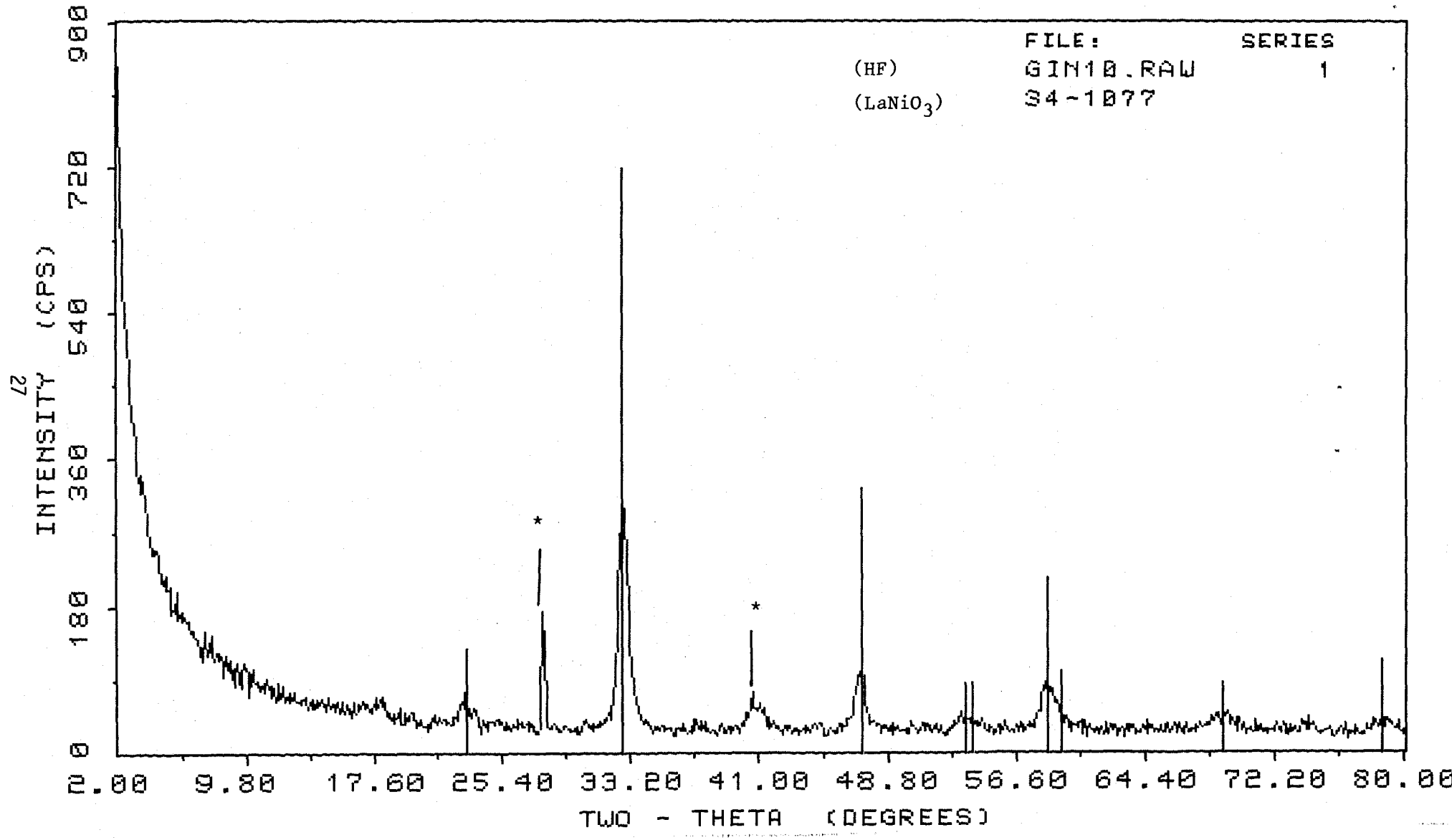

Figure 21. X-Ray Diffraction Pattern of $LaNiO_3$ Electrode after Bifunctional Testing

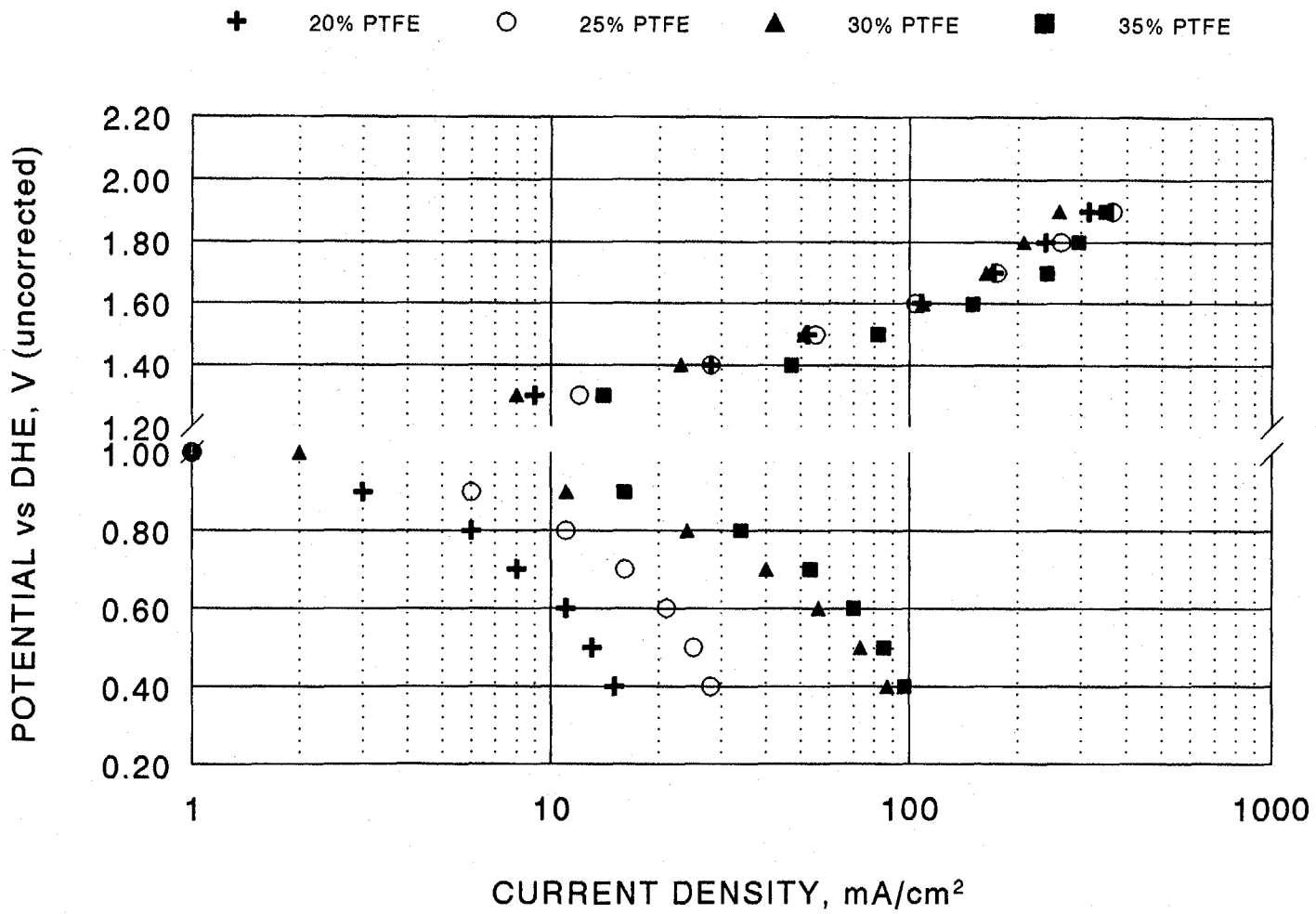

Figure 22. Oxygen Reduction/Evolution Performance of $LaNiO_3$ Electrodes in 30% KOH, 40°C

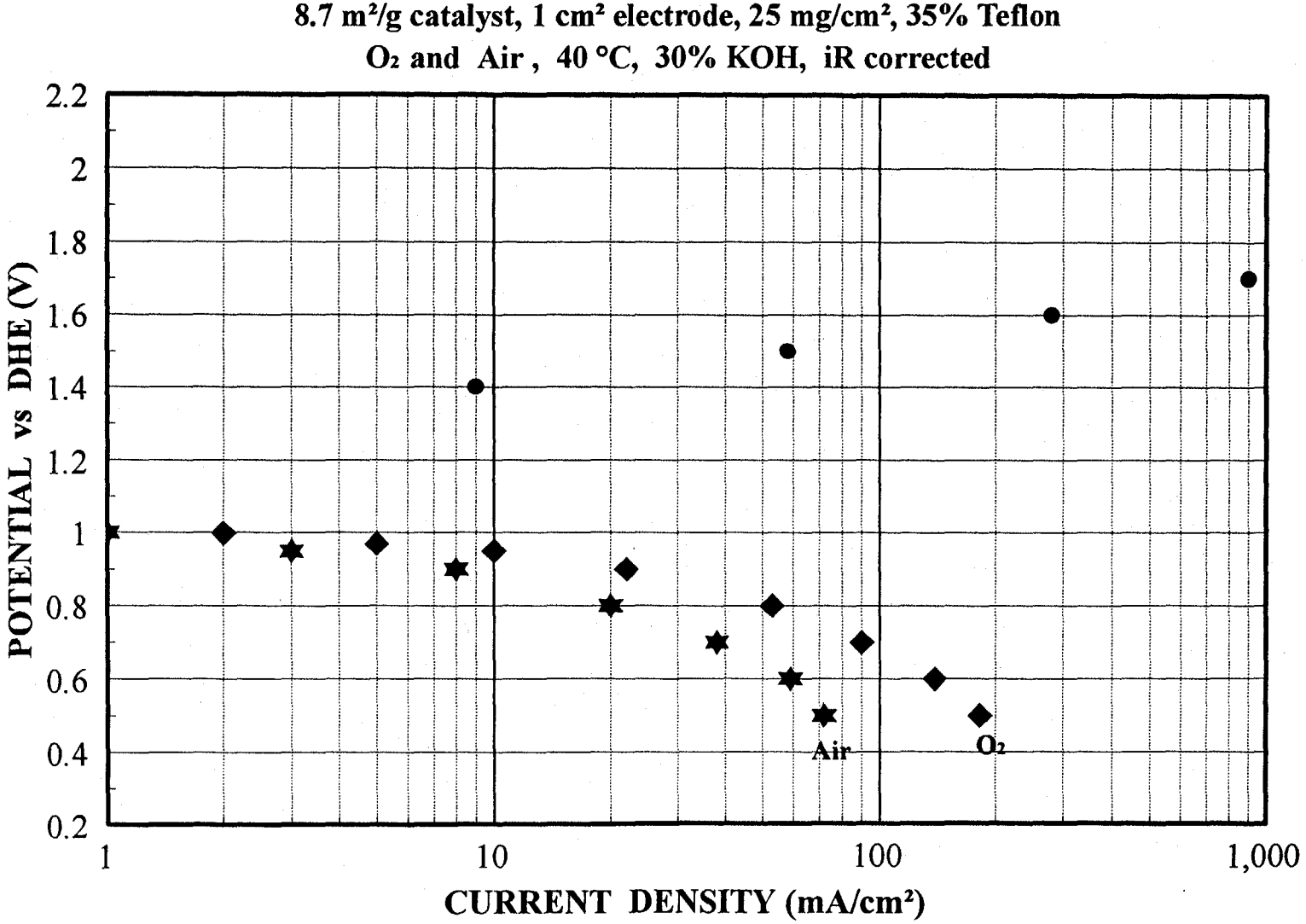

Figure 23. Bifunctional Performance of $LaNiO_3$ (HCP Preparation, 800°C, 6 hrs)

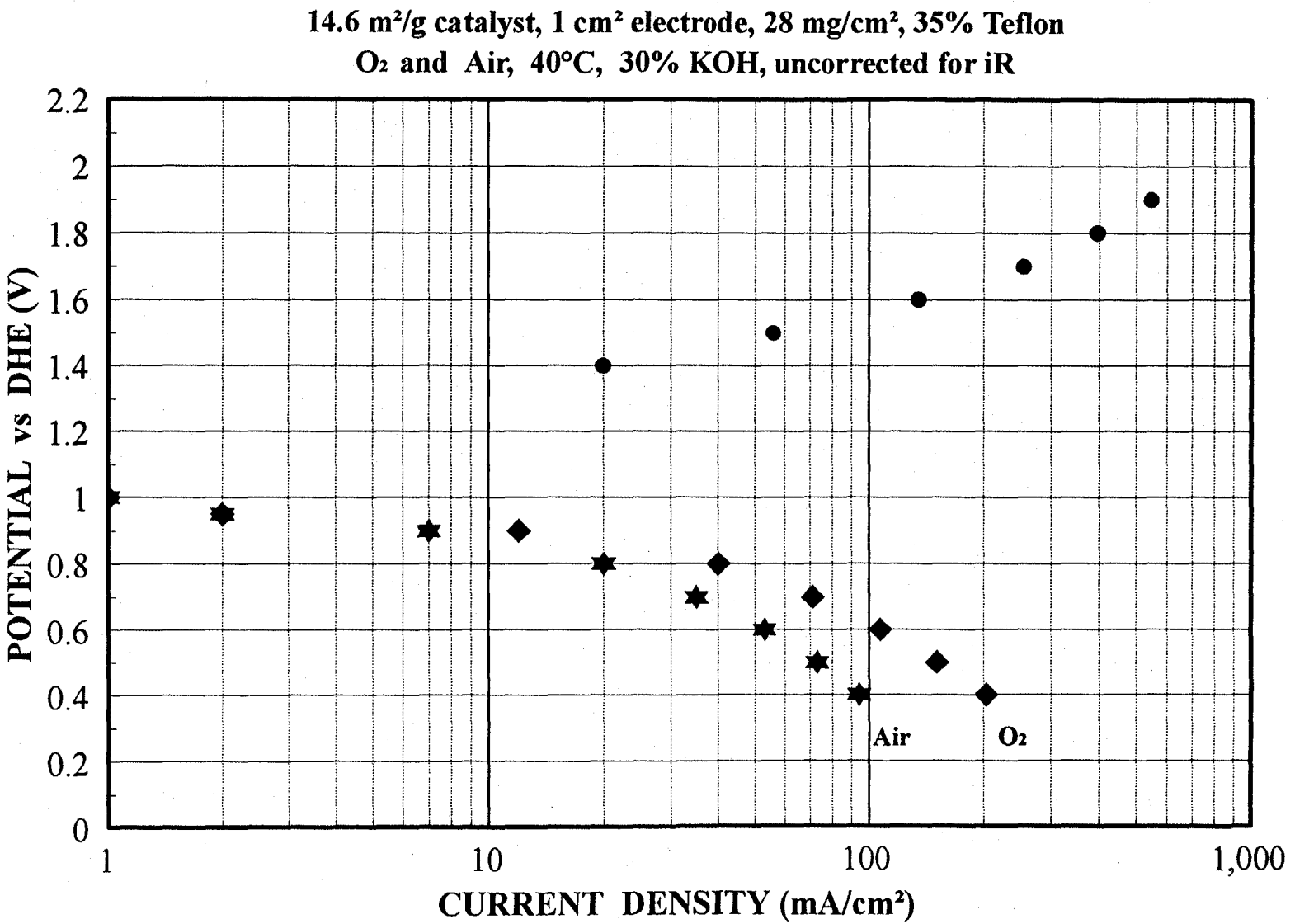

Figure 24. Bifunctional Performance of $LaNiO_3$ (HCP Method, 700°C, 6 hrs)

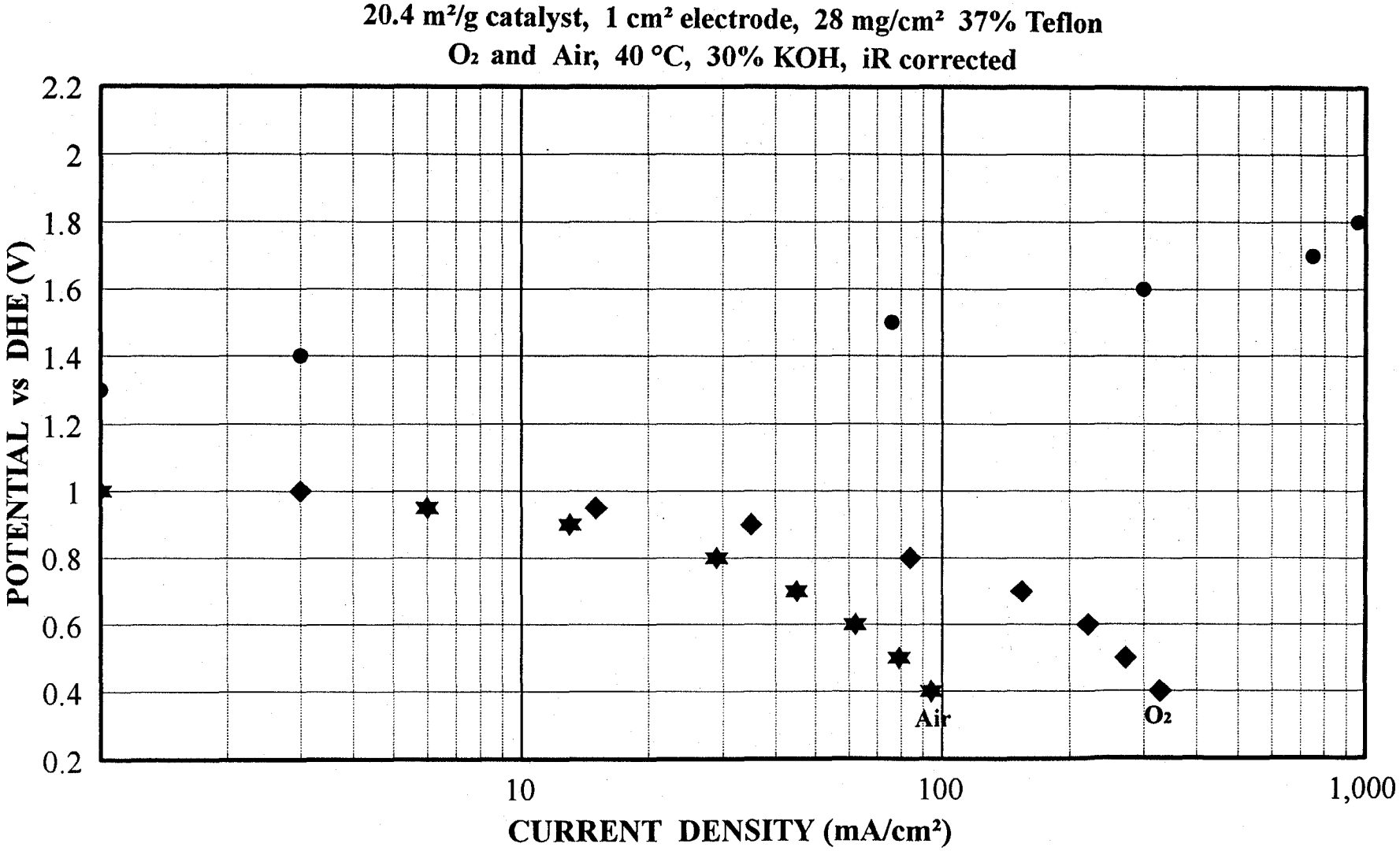

Figure 25. Bifunctional Performance of $LaNiO_3$ (HCP Method, 400°C/6 hrs + 600°C/6 hrs)

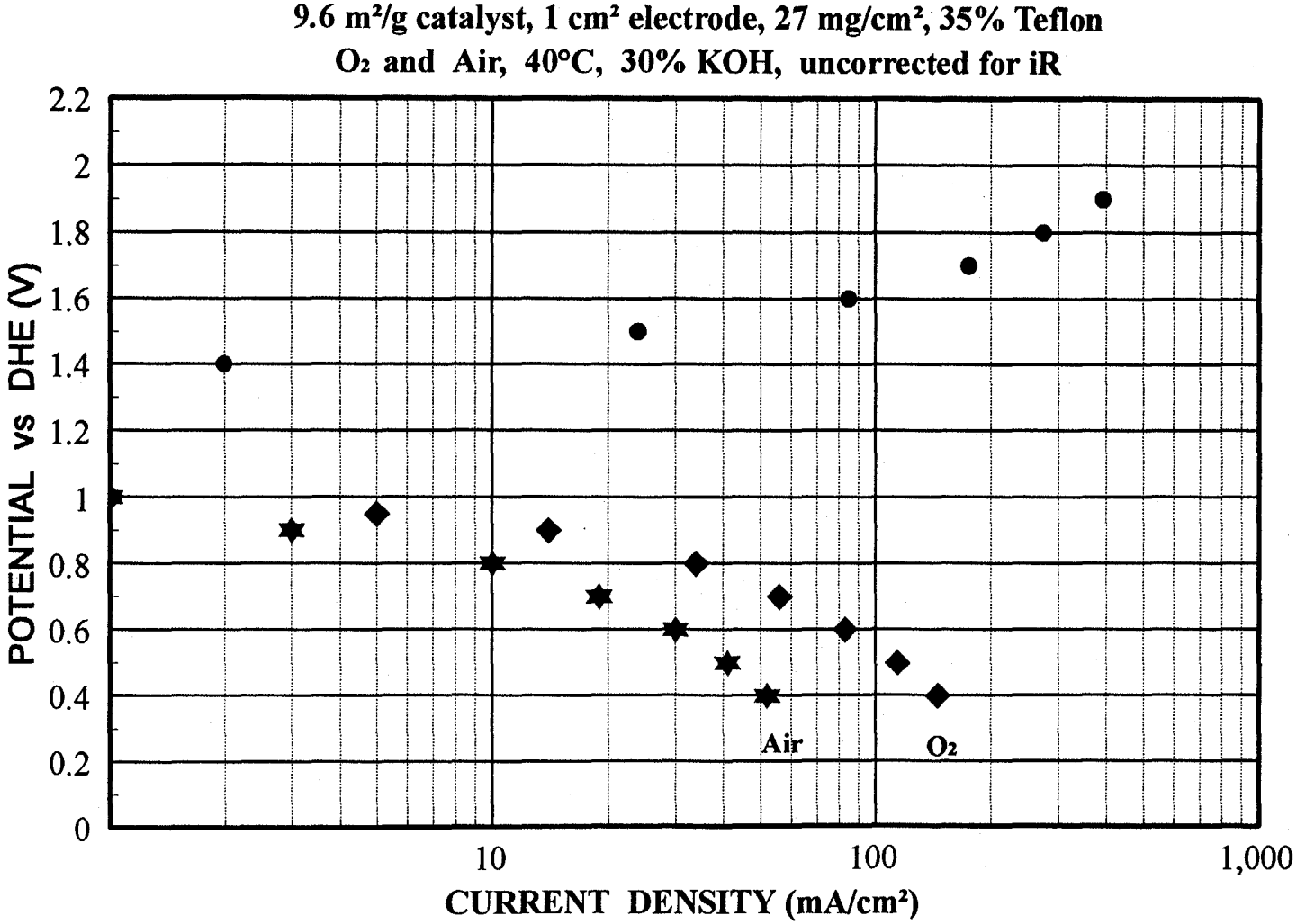

Figure 26. Bifunctional Performance of $LaNiO_3$ (ACP Method, 800°C, 2.5 hrs)

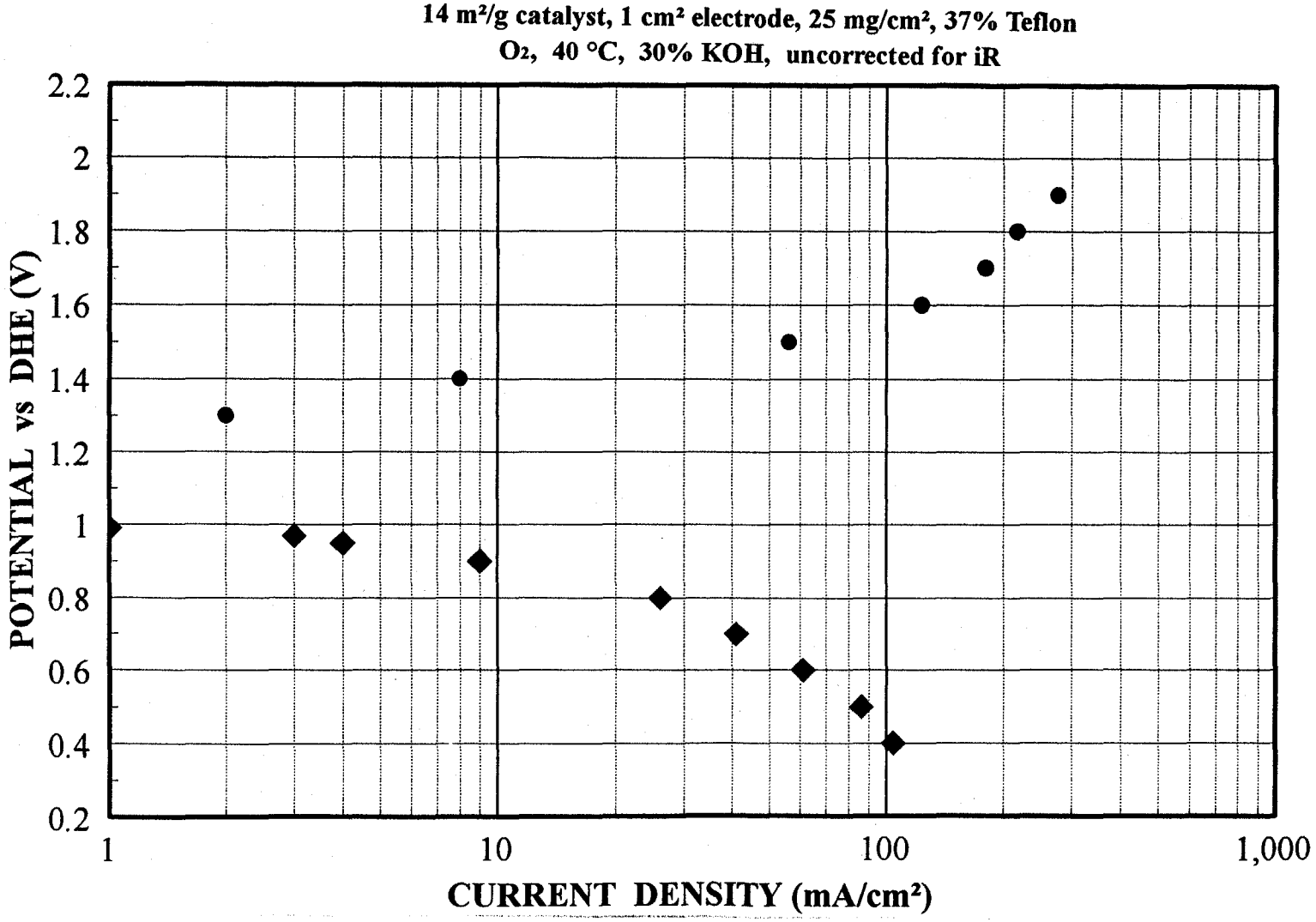

Figure 27. Bifunctional Performance of $La_{1-x}CaCoO_3$ (ACP Method, 600°C, 4 hrs)